

CONSERVATION OF S-CHANNEL HELICITY IN ρ^0 PHOTOPRODUCTION*

J. Ballam, G. B. Chadwick, R. Gearhart, Z. G. T. Guiragossian,
M. Menke, J. J. Murray, P. Seyboth,** A. Shapira, ***
C. K. Sinclair, I. O. Skillicorn,† and G. Wolf††

Stanford Linear Accelerator Center
Stanford University, Stanford, California 94305

R. H. Milburn

Tufts University, Medford, Massachusetts 02155

H. H. Bingham, W. B. Fretter, K. C. Moffeit, W. J. Podolsky,
M. S. Rabin, A. H. Rosenfeld, and R. Windmolders†††

Department of Physics and Lawrence Radiation Laboratory
University of California, Berkeley, California 94720

ABSTRACT

An analysis was made of the decay angular distribution of rho mesons produced via $\gamma p \rightarrow p \rho^0$ by linearly polarized photons at 2.8 and 4.7 GeV. The reaction proceeds almost completely through natural parity exchange, the contribution from unnatural parity exchange for momentum transfers $|t| < 1 \text{ GeV}^2$ being $3.1 \pm 2.2\%$ at 2.8 GeV and $-1.1 \pm 1.9\%$ at 4.7 GeV. The behavior of the density matrix elements shows that the rho production mechanism conserves s-channel c.m.s. helicity for $|t| < 0.4 \text{ GeV}^2$.

(Submitted to Phys. Rev. Letters)

* Work supported in part by the U. S. Atomic Energy Commission and the National Science Foundation.

** On leave from Max-Planck Institut für Physik und Astrophysik, Munich, Germany.

*** On leave from Weizmann Institute, Rehovoth, Israel.

† On leave from Brookhaven National Laboratory, Upton, New York.

†† On leave from DESY, Hamburg, Germany.

††† Visitor from Laboratoire Interuniversitaire des Hautes Energies, Brussels, Belgium.

Previous studies of ρ^0 production via $\gamma p \rightarrow p \rho^0$ have shown that the cross section is essentially constant above 2 GeV, a characteristic of diffractive processes, and that the transverse part of ρ^0 production is dominated by natural parity exchange;¹⁻⁵ also it has been indicated that s-channel c. m. s. helicity is conserved.² In this paper we establish that ρ^0 production is dominated by natural parity exchange and that it conserves s-channel c. m. s. helicity for $|t| < 0.4 \text{ GeV}^2$.

We studied rho production with linearly polarized photons by exposing the 82-inch hydrogen bubble chamber at SLAC to the monochromatic Compton back-scattered photon beam at 2.8 and 4.7 GeV. From 2854 events at 2.8 GeV and 2910 events at 4.7 GeV of the reaction



a sample of ~ 4000 ρ^0 events was obtained. Experimental details, mass distributions, a discussion of the ρ^0 mass shift, and ρ^0 production cross sections for reaction (1) are given elsewhere.⁶

In this paper we report the results from the study of the ρ^0 decay angular distribution. The analysis used the formalism of Ref. 7. We present the results in three reference systems which differ in the choice of the spin quantization axis (z axis): the Gottfried-Jackson system, where the z axis is chosen as the direction of the incident photon in the ρ^0 rest system; the helicity system where the z axis is opposite to the direction of the outgoing proton in the ρ^0 rest system; and the Adair system, where the z axis is along the direction of the incident photon in the overall c. m. system. The y axis is always normal to the production plane. For forward produced ρ^0 mesons, all three systems coincide.

We define the following angles⁸: ϕ is the angle of the photon electric polarization vector with respect to the production plane and is the same in the total c. m. s.

and the ρ^0 rest system; θ and ϕ are the polar and azimuthal angles of the π^+ in the ρ^0 rest system. The decay angular distribution for rho mesons produced by linearly polarized photons can be expressed in terms of nine independent measurable spin density matrix parameters ρ_{ik}^α (7, 9):

$$\begin{aligned}
W(\cos \theta, \phi, \Phi) = & \frac{3}{4\pi} \left\{ \frac{1}{2} (1 - \rho_{00}^0) + \frac{1}{2} (3\rho_{00}^0 - 1) \cos^2 \theta - \sqrt{2} \operatorname{Re} \rho_{10}^0 \sin 2\theta \cos \phi \right. \\
& - \rho_{1-1}^0 \sin^2 \theta \cos 2\phi - P_\gamma \cos 2\Phi \left[\rho_{11}^1 \sin^2 \theta + \rho_{00}^1 \cos^2 \theta \right. \\
& \left. \left. - \sqrt{2} \operatorname{Re} \rho_{10}^1 \sin 2\theta \cos \phi - \rho_{1-1}^1 \sin^2 \theta \cos 2\phi \right] \right. \\
& \left. - P_\gamma \sin 2\Phi \left[\sqrt{2} \operatorname{Im} \rho_{10}^2 \sin 2\theta \sin \phi + \operatorname{Im} \rho_{1-1}^2 \sin^2 \theta \sin 2\phi \right] \right\} \quad (2)
\end{aligned}$$

Here, P_γ is the degree of linear polarization of the photon, which is calculated from the Compton scattering process to be 94% at 2.8 GeV and 92% at 4.7 GeV. The matrix elements ρ_{ik}^0 describe the rho decay in the case of an unpolarized beam; the additional terms ρ_{ik}^1 and ρ_{ik}^2 result from the linear polarization of the photon.

Matters are simplified if we use the angle $\psi = \phi - \Phi$, which in the forward direction is the angle between the photon-polarization and ρ^0 decay planes. If the rho is transverse and linearly polarized like the photon then in the helicity system, $\rho_{1-1}^1 = -\operatorname{Im} \rho_{1-1}^2 = 1/2$ and all other ρ_{ik}^α in Eq. (2) are zero. In this case the decay angular distribution is proportional to $\sin^2 \theta \cos^2 \psi$. Note that under these conditions ψ becomes the azimuthal angle of the decay π^+ with respect to the rho polarization plane.

Figure 1 shows the distributions of the polar angle θ and the angle ψ in the helicity system for events in the rho mass region with $|t| < 0.4 \text{ GeV}^2$ where t is the square of the four-momentum transfer between incoming and outgoing proton.

The $\cos \theta$ distributions are proportional to $\sin^2 \theta$, i. e., the rho mesons are produced in reaction (1) with c. m. s. helicity ± 1 . The ψ distributions are $\sim \cos^2 \psi$ and show that the rho is almost completely linearly polarized.

The matrices ρ_{ik}^0 , ρ_{ik}^1 and ρ_{ik}^2 can be used to examine the production mechanism; for example, the contributions σ^N , σ^U from natural parity ($P = (-1)^J$) and unnatural parity ($P = -(-1)^J$) exchanges in the t-channel can be obtained by measuring P_σ ,

$$P_\sigma = \frac{\sigma^N - \sigma^U}{\sigma^N + \sigma^U} \quad (3)$$

which to leading order in energy is given by

$$P_\sigma = 2\rho_{1-1}^1 - \rho_{00}^1 \quad (4)$$

The expression (4) for P_σ is an invariant under rotations around the normal to the production plane.

We studied the influence of possible background by determining the ρ_{ik}^α as a function of the $\pi^+\pi^-$ mass, $M_{\pi\pi}$, with the method of moments using all events in a given $\pi^+\pi^-$ mass interval. Figure 2 shows the $M_{\pi\pi}$ dependence of ρ_{00}^0 and ρ_{1-1}^1 in the helicity system and that of P_σ . There is a pronounced difference between their values inside and outside of the rho region. The values $\rho_{00}^0 \cong 0$, $\rho_{1-1}^1 \cong 0.5$ and $P_\sigma \cong 1$ in the rho region are clearly associated with the production of the rho.

We took the background contribution into account by determining the rho density matrix parameters through a maximum likelihood fit including ρ^0 , Δ^{++} and phase space contributions.¹⁰ This method was checked by evaluating the ρ_{ik}^α inside and outside of the rho region and interpolating the contribution from the background. Within errors, the same result was obtained. Even if all events in the mass region $0.60 < M_{\pi\pi} < 0.85$ GeV are used without background subtraction the values of the ρ_{ik}^α do not change by more than one standard

deviation.¹¹ We conclude that the rho density matrix parameters are insensitive to the assumed form of the background.

In Fig. 3 P_σ is shown as a function of t . We see that rho production is completely dominated by natural parity exchange up to $|t| = 1 \text{ GeV}^2$. Averaging P_σ over the range $|t| \leq 1 \text{ GeV}^2$ we find the contribution from unnatural parity exchange to be $3.1 \pm 2.2\%$ at 2.8 GeV and $-1.1 \pm 1.9\%$ at 4.7 GeV.

In Fig. 3 we also display the quantity Σ defined as⁷

$$\Sigma = \frac{\sigma_{\parallel} - \sigma_{\perp}}{\sigma_{\parallel} + \sigma_{\perp}} = \frac{\rho_{11}^1 + \rho_{1-1}^1}{\rho_{11}^0 + \rho_{1-1}^0} \quad (5)$$

which has been measured in counter experiments. Here σ_{\parallel} and σ_{\perp} are the cross sections for the pions from symmetric rho decay to emerge in the plane of the photon polarization and perpendicular to it ($\theta = \pi/2$, $\phi = \pi/2$, $\Phi = 0, \pi/2$). Our values of Σ at 2.8 GeV are in agreement with measurements at 2.4 GeV made at DESY.^{5, 12}

Finally, Fig. 4 and Table I show the density matrix parameters themselves, evaluated in the Gottfried-Jackson, helicity and Adair systems as a function of t . We note that the density matrix elements can be expressed in terms of bilinear combinations of helicity or spin amplitudes and that, for example, ρ_{00}^0 and ρ_{00}^1 receive only contributions from helicity-flip or spin-flip amplitudes.

We conclude from the behavior of the ρ_{ik}^α :

1. The density matrix parameters vary rapidly in the Gottfried-Jackson system.^{1, 13} The t-channel helicity-flip amplitudes increase rapidly with increasing $|t|$. This behavior rules out t-channel helicity conservation and also excludes a zero spin particle exchange without absorption as the only contributor to rho production.

2. The ρ_{ik}^α in the Adair system also vary significantly with t (see also Fig. 5a). This excludes² the hypothesis of spin independence in the total c. m. system for rho production.¹³

3. In the helicity system the helicity-flip contributions are zero within errors up to $|t| = 0.4 \text{ GeV}^2$, i. e., the rho behaves like a photon with the spin aligned along its direction of motion. In other words, the rho production mechanism conserves s-channel c. m. s. helicity. The fact that the flip contributions are minimum in the helicity system is further demonstrated in Figs. 5b, c. The rho density matrix as calculated in the helicity frame was rotated by an angle β around the production normal and a least squares fit made to find that value of β for which the flip terms become minimal, i. e., for which the rho density matrix is closest to that of the photon (see above). Figs. 5b, c show β as a function of the rho c. m. s. production angle θ_{cm} together with lines indicating where the data points should fall if the flip terms were minimal in the Gottfried-Jackson (G.J.), helicity (H), or Adair system (A), respectively. For $\theta_{\text{cm}} \lesssim 25^\circ$, the helicity system is clearly preferred.

In summary, rho photoproduction via $\gamma p \rightarrow p\rho^0$ proceeds almost completely through natural parity exchange and conserves helicity in the s-channel c. m. system up to $|t| = 0.4 \text{ GeV}^2$. We remark that these features may be general characteristics of diffraction scattering.¹⁴

ACKNOWLEDGEMENTS

We wish to thank the SLAC operations crew of the accelerator and R. Watt and the 82" bubble-chamber operation group. We acknowledge the diligent work of the scanners at SLAC and Berkeley and in particular the help in data reduction by K. Eymann and W. Hendricks.

REFERENCES AND FOOTNOTES

1. Cambridge Bubble Chamber Group, Phys. Rev. 146, 994 (1966).
2. Aachen-Berlin-Bonn-Hamburg-Heidelberg-München Collaboration, Phys. Rev. 175, 1669 (1968).
3. R. Anderson et al., Report No. SLAC-PUB-644, Stanford Linear Accelerator Center, (1969) (to be published in Phys. Rev.).
4. See also work quoted by A. Silverman, Proceedings of the 4th International Symposium on Electron and Photon Interactions at High Energies, Liverpool, (1969), edited by D. W. Braben, p. 71.
5. L. Criegee et al., Phys. Letters 28B, 282 (1968). (See also the data of these authors as quoted by E. Lohrmann, Rapporteur's talk, Lund Conference June 1969, and DESY Report No. 69-21 (1969)).
6. SLAC-Berkeley-Tufts Collaboration, "The reaction $\gamma p \rightarrow p \rho^0$ with linearly polarized photons at 2.8 and 4.7 GeV: cross section measurements and the ρ mass shift," (to be published).
7. K. Schilling, P. Seyboth, and G. Wolf, Report No. SLAC-PUB-683, Stanford Linear Accelerator Center (to be published in Nucl. Phys.).
8. The y axis is the normal to the production plane, defined by the cross product $\hat{k} \times \hat{\rho}$ of the directions of the photon and the vector meson. The x axis is given by $\hat{x} = \hat{y} \times \hat{z}$. The angle Φ between the electric vector of the photon, ϵ , and the production plane in the total c. m. system is defined by: $\cos \Phi = \hat{k} \cdot (\hat{\epsilon} \times \hat{y})$, $\sin \Phi = \hat{y} \cdot \hat{\epsilon}$. The decay angles θ , ϕ are the polar and azimuthal angles of the direction of flight of the π^+ in the ρ rest system:

$$\cos \theta = \hat{\pi} \cdot \hat{z}$$

$$\cos \phi = \hat{y} \cdot (\hat{z} \times \hat{\pi}) / |\hat{z} \times \hat{\pi}|$$

$$\sin \phi = -\hat{x} \cdot (\hat{z} \times \hat{\pi}) / |\hat{z} \times \hat{\pi}|$$

9. R. L. Thews, Phys. Rev. 175, 1749 (1968).

10. The following Dalitz plot density distribution has been used:

$$\frac{a_\rho}{N_\rho} B_\rho W(\cos \theta, \phi, \Phi) \cdot F_\rho(t) + \frac{a_\Delta}{N_\Delta} B_\Delta F_\Delta(t_\Delta) + \frac{a_{ps}}{N_{ps}} B_{ps}$$

Here t_Δ is the square of the four momentum transfer between incoming proton and outgoing Δ^{++} (1236); a_ρ , a_Δ , and a_{ps} are the fractions of ρ^0 , Δ^{++} (1236) and phase space distributed events; B_ρ is a p-wave Breit-Wigner distribution for the ρ^0 multiplied by a factor $(m_\rho/M_{\pi\pi})^4$ (see Ref. 2 for discussion); B_Δ is a p-wave Breit-Wigner for the Δ^{++} (1236); $B_{ps} = \text{const}$ is the Lorentz invariant phase space distribution; $F_\rho(t)$ and $F_\Delta(t)$ have been empirically determined and describe the t distributions for ρ^0 and Δ^{++} production; N_ρ , N_Δ and N_{ps} are normalization factors. In these fits the values of the ρ_{ik}^α were not constrained. Consequently P_σ and Σ may be greater than unity.

11. A further check on the influence of the background on the values of the ρ_{ik}^α was made by using the Söding model, which has been found to describe ρ^0 production (Ref. 6). We have evaluated the Söding model assuming for the ρ^0 production the values obtained from the maximum likelihood fit for the density matrix parameters. An analysis of the resulting $\pi^+\pi^-$ angular distributions shows that the Drell term has no significant influence on the decay angular distribution of the rho.

12. Σ has also been measured by Diambri-Palazzi et al., as quoted in Ref. 4.

13. This assumption was made in the "strong absorption model", Y. Eisenberg, et al., Phys. Letters 22, 217 (1966); 22, 223 (1966); see also G. Kramer, DESY Report No. 67/32, (1967) (unpublished).

14. See also F. J. Gilman, J. Pumplin, A. Schwimmer, and L. Stodolsky, Report No. SLAC-PUB-719, Stanford Linear Accelerator Center (1970), submitted to Phys. Letters.

TABLE I

Rho-Density Matrix Elements for the Reaction $\gamma p \rightarrow p \rho^0$ a) $E_\gamma = 2.8$ GeV, Gottfried-Jackson system

$ t (\text{GeV}^2)$	0.02 - 0.05	0.05 - 0.08	0.08 - 0.12	0.12 - 0.18	0.18 - 0.25	0.25 - 0.40	0.4 - 1.0
ρ_{00}^0	0.079 ± 0.030	0.119 ± 0.035	0.298 ± 0.041	0.431 ± 0.047	0.455 ± 0.051	0.525 ± 0.052	0.476 ± 0.071
$\text{Re}\rho_{10}^0$	0.143 ± 0.019	0.195 ± 0.023	0.180 ± 0.020	0.158 ± 0.024	0.146 ± 0.027	-0.002 ± 0.027	-0.089 ± 0.046
ρ_{1-1}^0	0.151 ± 0.037	0.112 ± 0.035	0.111 ± 0.033	0.161 ± 0.035	0.160 ± 0.037	0.267 ± 0.038	0.071 ± 0.057
ρ_{00}^1	-0.140 ± 0.056	-0.057 ± 0.048	-0.231 ± 0.071	-0.328 ± 0.081	-0.390 ± 0.085	-0.359 ± 0.094	-0.483 ± 0.118
ρ_{11}^1	0.091 ± 0.040	0.048 ± 0.045	0.092 ± 0.040	0.114 ± 0.037	0.208 ± 0.042	0.212 ± 0.045	0.134 ± 0.067
$\text{Re}\rho_{10}^1$	-0.085 ± 0.035	-0.170 ± 0.033	-0.167 ± 0.029	-0.113 ± 0.037	-0.111 ± 0.042	-0.059 ± 0.042	0.119 ± 0.067
ρ_{1-1}^1	0.505 ± 0.045	0.414 ± 0.055	0.358 ± 0.039	0.270 ± 0.046	0.258 ± 0.047	0.125 ± 0.060	0.246 ± 0.088
$\text{Im}\rho_{10}^2$	0.136 ± 0.035	0.249 ± 0.040	0.229 ± 0.032	0.274 ± 0.034	0.259 ± 0.042	0.341 ± 0.033	0.094 ± 0.073
$\text{Im}\rho_{1-1}^2$	-0.462 ± 0.036	-0.417 ± 0.053	-0.254 ± 0.058	-0.240 ± 0.054	-0.244 ± 0.058	-0.046 ± 0.040	-0.095 ± 0.091

Table I (cont'd.) - 2

b) $E_\gamma = 2.8$ GeV, helicity system

$ t (\text{GeV}^2)$	0.02 - 0.05	0.05 - 0.08	0.08 - 0.12	0.12 - 0.18	0.18 - 0.25	0.25 - 0.40	0.4 - 1.0
ρ_{00}^0	-0.045 ± 0.030	-0.034 ± 0.033	0.021 ± 0.029	0.026 ± 0.036	0.016 ± 0.042	-0.071 ± 0.042	0.173 ± 0.064
$\text{Re}\rho_{10}^0$	0.013 ± 0.018	-0.032 ± 0.020	0.008 ± 0.023	0.026 ± 0.027	-0.028 ± 0.026	0.112 ± 0.027	0.140 ± 0.043
ρ_{1-1}^0	0.078 ± 0.037	0.027 ± 0.040	-0.024 ± 0.041	-0.045 ± 0.040	-0.052 ± 0.048	-0.001 ± 0.047	-0.079 ± 0.060
ρ_{00}^1	-0.061 ± 0.056	0.018 ± 0.059	-0.036 ± 0.047	-0.015 ± 0.055	0.041 ± 0.059	0.172 ± 0.063	-0.088 ± 0.108
ρ_{11}^1	0.042 ± 0.046	0.001 ± 0.050	-0.008 ± 0.042	-0.049 ± 0.050	-0.011 ± 0.054	-0.050 ± 0.061	-0.073 ± 0.079
$\text{Re}\rho_{10}^1$	0.015 ± 0.030	0.071 ± 0.030	0.026 ± 0.037	-0.009 ± 0.039	0.004 ± 0.037	-0.037 ± 0.042	-0.138 ± 0.062
ρ_{1-1}^1	0.539 ± 0.044	0.453 ± 0.052	0.458 ± 0.043	0.427 ± 0.050	0.484 ± 0.064	0.355 ± 0.062	0.457 ± 0.085
$\text{Im}\rho_{10}^2$	-0.050 ± 0.034	0.012 ± 0.040	0.012 ± 0.034	0.016 ± 0.037	-0.073 ± 0.044	0.036 ± 0.031	-0.070 ± 0.064
$\text{Im}\rho_{1-1}^2$	-0.496 ± 0.039	-0.551 ± 0.053	-0.427 ± 0.054	-0.445 ± 0.049	-0.424 ± 0.058	-0.465 ± 0.043	-0.157 ± 0.101

Table I (cont'd.) - 3

c) $E_\gamma = 2.8$ GeV, Adair systems

$ t (\text{GeV}^2)$	0.02 - 0.05	0.05 - 0.08	0.08 - 0.12	0.12 - 0.18	0.18 - 0.25	0.25 - 0.40	0.4 - 1.0
ρ_{00}^0	-0.023 ± 0.029	-0.029 ± 0.033	0.066 ± 0.032	0.114 ± 0.043	0.084 ± 0.040	0.238 ± 0.040	0.512 ± 0.073
$\text{Re}\rho_{10}^0$	0.063 ± 0.019	0.060 ± 0.019	0.104 ± 0.022	0.141 ± 0.023	0.129 ± 0.030	0.237 ± 0.030	0.115 ± 0.041
ρ_{1-1}^0	0.088 ± 0.037	0.030 ± 0.040	-0.002 ± 0.039	-0.001 ± 0.039	-0.020 ± 0.045	0.152 ± 0.045	0.091 ± 0.055
ρ_{00}^1	-0.071 ± 0.055	0.039 ± 0.054	-0.052 ± 0.054	-0.084 ± 0.071	-0.054 ± 0.056	-0.027 ± 0.071	-0.442 ± 0.123
ρ_{11}^1	0.048 ± 0.044	-0.009 ± 0.049	0.001 ± 0.042	-0.015 ± 0.049	0.038 ± 0.050	0.051 ± 0.048	0.105 ± 0.066
$\text{Re}\rho_{10}^1$	-0.026 ± 0.033	-0.019 ± 0.031	-0.064 ± 0.034	-0.114 ± 0.034	-0.148 ± 0.044	-0.202 ± 0.046	-0.168 ± 0.062
ρ_{1-1}^1	0.531 ± 0.043	0.464 ± 0.053	0.450 ± 0.043	0.392 ± 0.049	0.438 ± 0.059	0.258 ± 0.063	0.276 ± 0.087
$\text{Im}\rho_{10}^2$	0.008 ± 0.035	0.096 ± 0.041	0.099 ± 0.032	0.132 ± 0.035	0.063 ± 0.044	0.195 ± 0.035	0.007 ± 0.074
$\text{Im}\rho_{1-1}^2$	-0.499 ± 0.038	-0.531 ± 0.051	-0.405 ± 0.056	-0.404 ± 0.051	-0.427 ± 0.058	-0.372 ± 0.035	-0.155 ± 0.086

Table I (cont'd.) - 4

d) $E_\gamma = 4.7$ GeV, Gottfried-Jackson system

$ t (\text{GeV}^2)$	0.02 - 0.05	0.05 - 0.08	0.08 - 0.12	0.12 - 0.18	0.18 - 0.25	0.25 - 0.40	0.4 - 1.0
ρ_{00}^0	0.143 ± 0.029	0.227 ± 0.036	0.312 ± 0.038	0.357 ± 0.033	0.474 ± 0.047	0.577 ± 0.044	0.476 ± 0.064
$\text{Re}\rho_{10}^0$	0.158 ± 0.016	0.234 ± 0.020	0.148 ± 0.021	0.167 ± 0.019	0.114 ± 0.022	0.017 ± 0.027	-0.029 ± 0.036
ρ_{1-1}^0	0.066 ± 0.029	0.082 ± 0.033	0.133 ± 0.032	0.148 ± 0.030	0.229 ± 0.036	0.199 ± 0.026	0.077 ± 0.048
ρ_{00}^1	-0.172 ± 0.041	-0.187 ± 0.054	-0.245 ± 0.060	-0.315 ± 0.056	-0.554 ± 0.063	-0.338 ± 0.085	-0.377 ± 0.095
ρ_{11}^1	0.061 ± 0.037	0.083 ± 0.038	0.119 ± 0.036	0.147 ± 0.031	0.193 ± 0.035	0.195 ± 0.036	0.157 ± 0.048
$\text{Re}\rho_{10}^1$	-0.117 ± 0.028	-0.179 ± 0.029	-0.159 ± 0.029	-0.196 ± 0.033	-0.186 ± 0.028	-0.111 ± 0.045	0.064 ± 0.051
ρ_{1-1}^1	0.521 ± 0.037	0.302 ± 0.044	0.416 ± 0.038	0.302 ± 0.037	0.259 ± 0.049	0.273 ± 0.041	0.269 ± 0.059
$\text{Im}\rho_{10}^2$	0.152 ± 0.026	0.202 ± 0.029	0.277 ± 0.033	0.301 ± 0.025	0.305 ± 0.036	0.249 ± 0.039	0.256 ± 0.051
$\text{Im}\rho_{1-1}^2$	-0.326 ± 0.044	-0.413 ± 0.042	-0.343 ± 0.043	-0.278 ± 0.037	-0.158 ± 0.047	-0.090 ± 0.051	0.164 ± 0.076

Table I (cont'd.) - 5

e) $E_\gamma = 4.7$ GeV, helicity system

$ t (\text{GeV}^2)$	0.02 - 0.05	0.05 - 0.08	0.08 - 0.12	0.12 - 0.18	0.18 - 0.25	0.25 - 0.40	0.4 - 1.0
ρ_{00}^0	-0.009 ± 0.022	-0.037 ± 0.025	0.027 ± 0.031	0.021 ± 0.029	-0.002 ± 0.035	0.062 ± 0.028	0.208 ± 0.054
$\text{Re}\rho_{10}^0$	0.009 ± 0.018	0.001 ± 0.019	0.010 ± 0.023	-0.024 ± 0.019	0.031 ± 0.023	0.067 ± 0.027	0.043 ± 0.037
ρ_{1-1}^0	-0.001 ± 0.031	-0.064 ± 0.041	-0.003 ± 0.035	-0.031 ± 0.033	-0.006 ± 0.044	-0.052 ± 0.042	-0.048 ± 0.056
ρ_{00}^1	-0.087 ± 0.038	0.052 ± 0.032	-0.051 ± 0.043	-0.001 ± 0.045	0.054 ± 0.045	-0.049 ± 0.057	-0.140 ± 0.078
ρ_{11}^1	0.018 ± 0.039	-0.035 ± 0.041	0.025 ± 0.039	-0.020 ± 0.039	-0.105 ± 0.047	0.048 ± 0.048	0.040 ± 0.055
$\text{Re}\rho_{10}^1$	0.033 ± 0.027	-0.022 ± 0.028	-0.001 ± 0.037	0.008 ± 0.028	-0.007 ± 0.028	0.018 ± 0.046	-0.076 ± 0.053
ρ_{1-1}^1	0.548 ± 0.039	0.420 ± 0.054	0.521 ± 0.036	0.484 ± 0.038	0.563 ± 0.050	0.434 ± 0.051	0.390 ± 0.065
$\text{Im}\rho_{10}^2$	0.014 ± 0.024	-0.023 ± 0.030	-0.002 ± 0.027	-0.028 ± 0.028	0.009 ± 0.031	-0.007 ± 0.039	0.099 ± 0.056
$\text{Im}\rho_{1-1}^2$	-0.388 ± 0.047	-0.475 ± 0.042	-0.508 ± 0.047	-0.510 ± 0.038	-0.470 ± 0.051	-0.344 ± 0.054	-0.366 ± 0.069

Table I (cont'd.) - 6

f) $E_\gamma = 4.7$ GeV, Adair system

$ t $ (GeV ²)	0.02 - 0.05	0.05 - 0.08	0.08 - 0.12	0.12 - 0.18	0.18 - 0.25	0.25 - 0.40	0.4 - 1.0
ρ_{00}^0	0.005 ± 0.023	-0.014 ± 0.028	0.059 ± 0.032	0.044 ± 0.030	0.079 ± 0.038	0.207 ± 0.041	0.320 ± 0.056
$\text{Re}\rho_{10}^0$	0.056 ± 0.017	0.078 ± 0.019	0.081 ± 0.023	0.074 ± 0.018	0.135 ± 0.023	0.170 ± 0.021	0.092 ± 0.035
ρ_{1-1}^0	0.005 ± 0.031	-0.054 ± 0.040	0.014 ± 0.034	-0.022 ± 0.033	0.036 ± 0.042	0.021 ± 0.040	0.002 ± 0.056
ρ_{00}^1	-0.086 ± 0.038	0.017 ± 0.038	-0.073 ± 0.045	-0.032 ± 0.050	-0.030 ± 0.047	-0.072 ± 0.077	-0.296 ± 0.078
ρ_{11}^1	0.017 ± 0.039	-0.019 ± 0.041	0.035 ± 0.038	-0.003 ± 0.039	0.059 ± 0.045	-0.061 ± 0.047	0.120 ± 0.052
$\text{Re}\rho_{10}^1$	-0.008 ± 0.028	-0.085 ± 0.028	-0.067 ± 0.036	-0.084 ± 0.027	-0.162 ± 0.028	-0.072 ± 0.040	-0.105 ± 0.048
ρ_{1-1}^1	0.550 ± 0.038	0.405 ± 0.053	0.507 ± 0.037	0.466 ± 0.038	0.519 ± 0.050	0.419 ± 0.050	0.306 ± 0.072
$\text{Im}\rho_{10}^2$	0.049 ± 0.024	0.036 ± 0.030	0.078 ± 0.029	0.070 ± 0.027	0.114 ± 0.031	0.091 ± 0.040	0.225 ± 0.056
$\text{Im}\rho_{1-1}^2$	-0.382 ± 0.047	-0.472 ± 0.042	-0.498 ± 0.046	-0.499 ± 0.040	-0.441 ± 0.050	-0.320 ± 0.052	-0.233 ± 0.072

FIGURE CAPTIONS

1. Reaction $\gamma p \rightarrow p \rho^0$. Rho decay angular distributions in the helicity system for $|t| < 0.4 \text{ GeV}^2$ and $0.6 < M_{\pi\pi} < 0.85 \text{ GeV}$ without background subtraction. The curves for the $\cos\theta$ distributions are proportional to $\sin^2\theta$.
2. Reaction $\gamma p \rightarrow p \pi^+ \pi^-$. The density matrix elements ρ_{00}^0 and ρ_{1-1}^1 and the parity asymmetry, P_σ , as a function of $M_{\pi\pi}$.
3. Reaction $\gamma p \rightarrow p \rho^0$. The parity asymmetry, P_σ , and the asymmetry, Σ , as a function of t in the Gottfried-Jackson, helicity and Adair systems.
4. Reaction $\gamma p \rightarrow p \rho^0$. The spin density matrix parameters as a function of t in the Gottfried-Jackson, helicity and Adair systems.
5. Reaction $\gamma p \rightarrow p \rho^0$. (a) Comparison of the spin density matrix parameters ρ_{00}^0 , $\text{Re } \rho_{10}^0$, $\text{Re } \rho_{10}^1$, $\text{Im } \rho_{10}^2$ in the helicity (\downarrow) and Adair systems (\downarrow) as a function of t (data of Fig. 4). (b, c) The angle β for rotation into the "minimum flip" system as a function of the c. m. s. rho production angle θ_{cm} . For the curves labeled G.J., A, and H, see text.

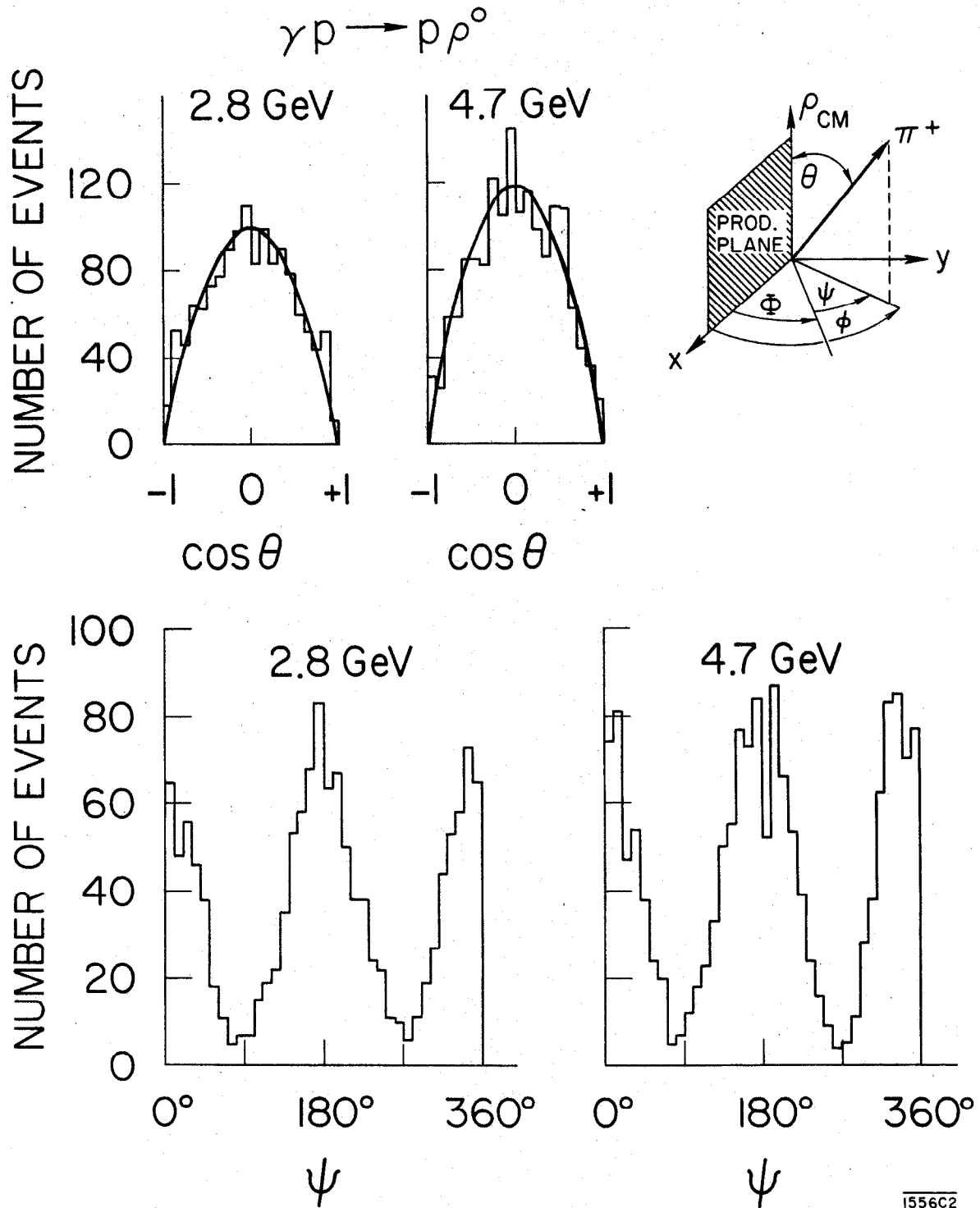


Fig. 1

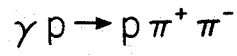
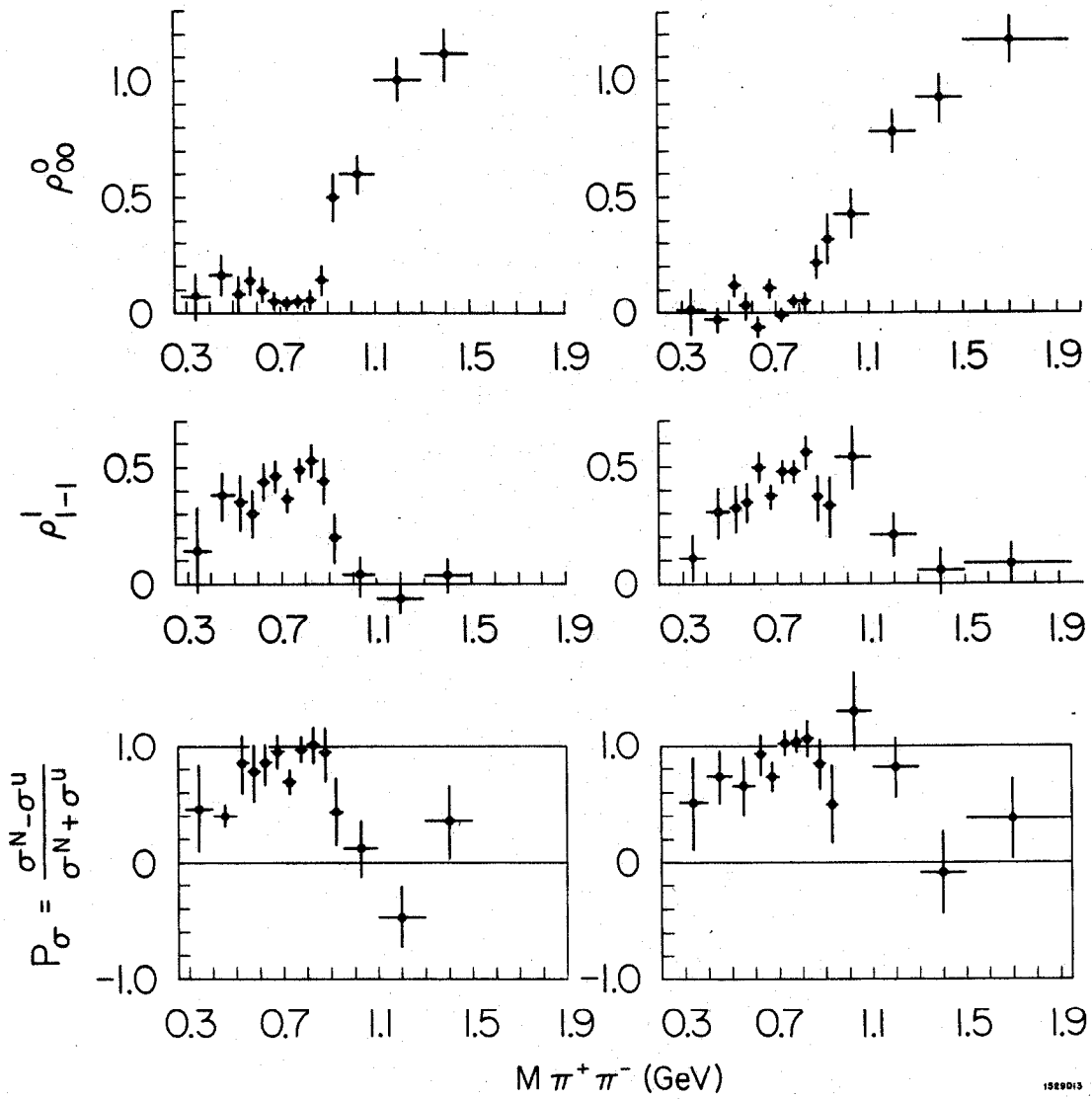
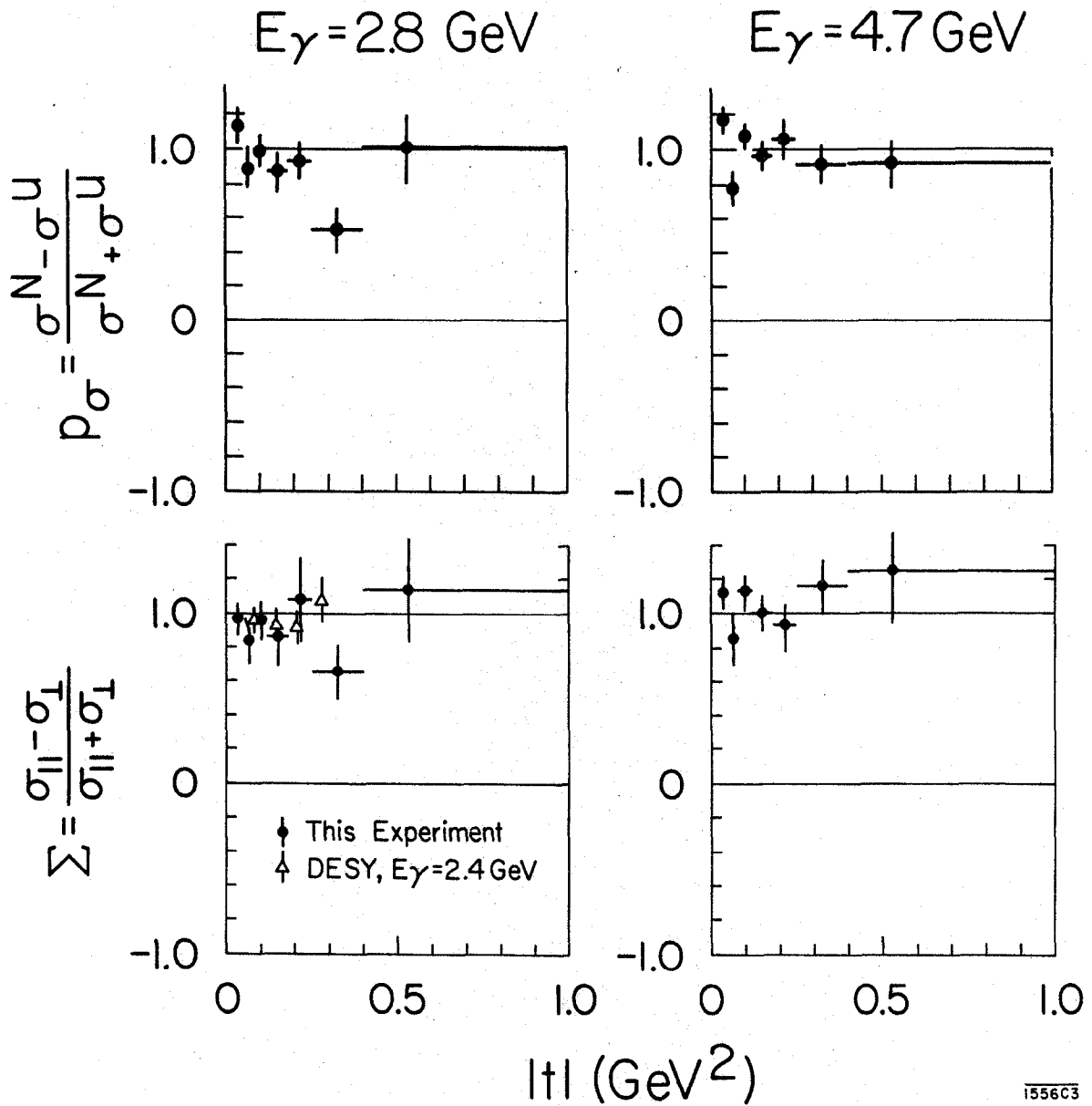
 $E_\gamma = 2.8 \text{ GeV}$ $E_\gamma = 4.7 \text{ GeV}$ $|t| < 0.4 \text{ GeV}^2$ 

Fig. 2



1556C3

Fig. 3

2.8 GeV $\gamma p \rightarrow p \rho^0$
 G.-J. HELICITY ADAIR

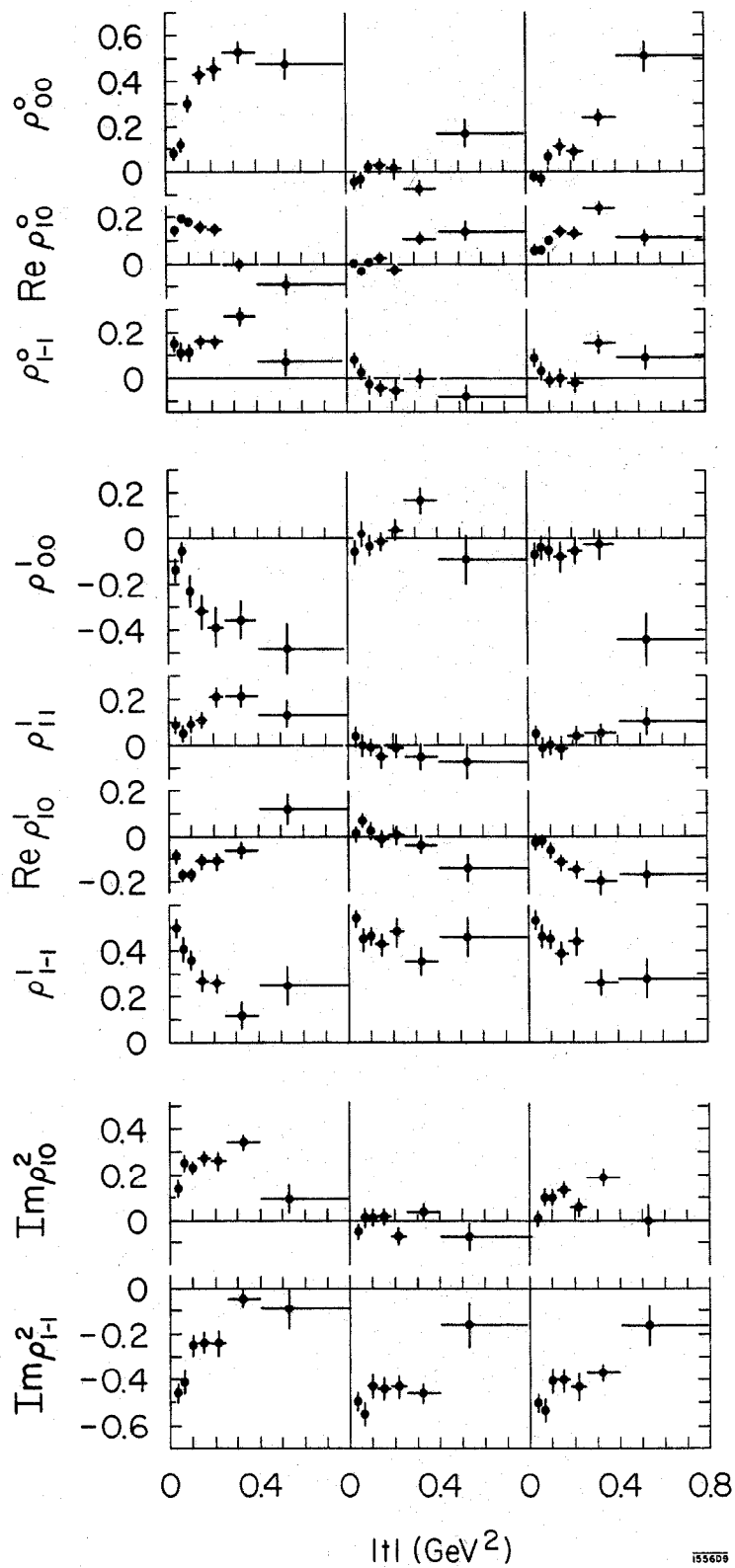


Fig. 4a

4.7 GeV $\gamma p \rightarrow p \rho^0$

G.-J. HELICITY ADAIR

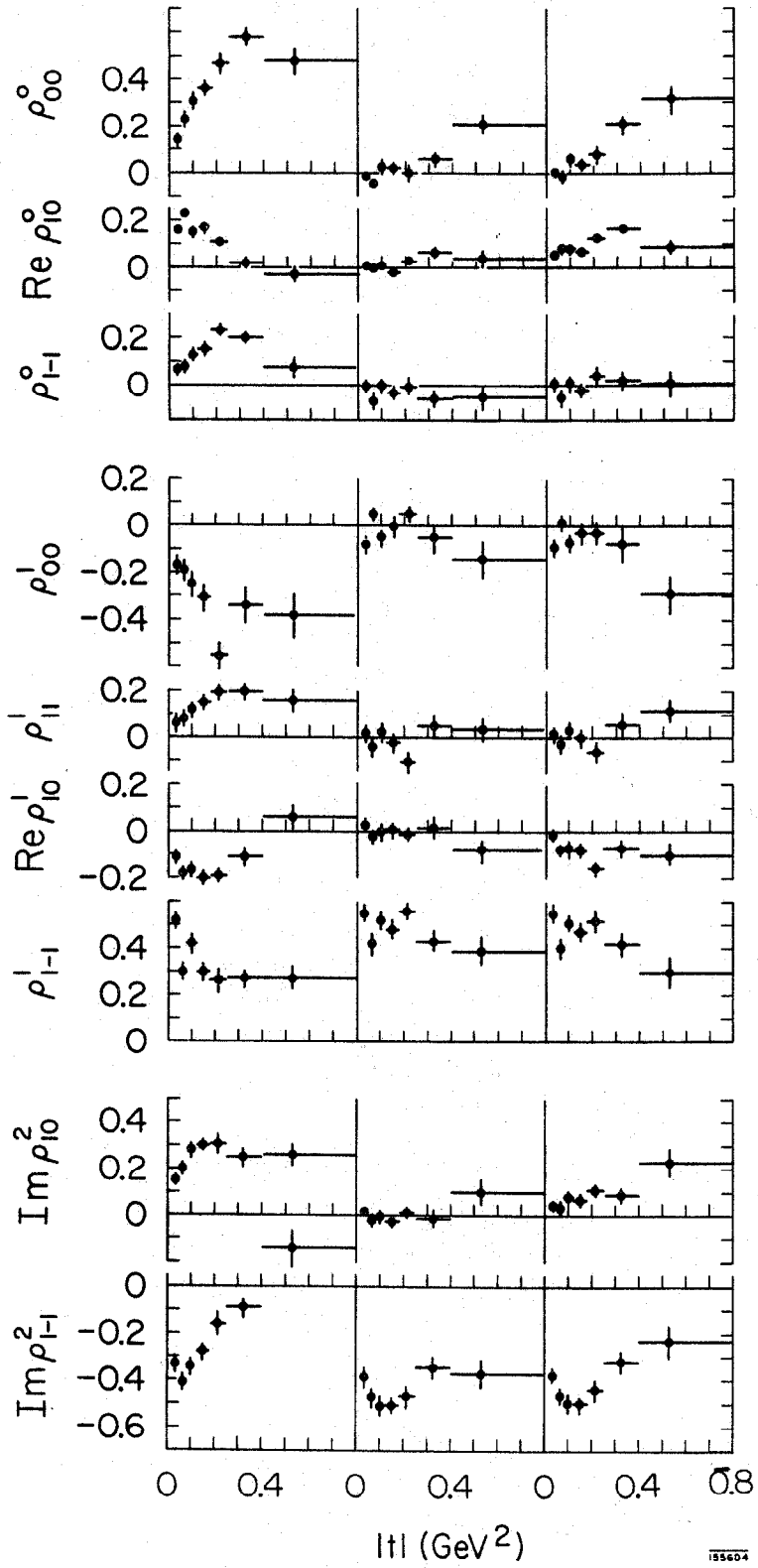
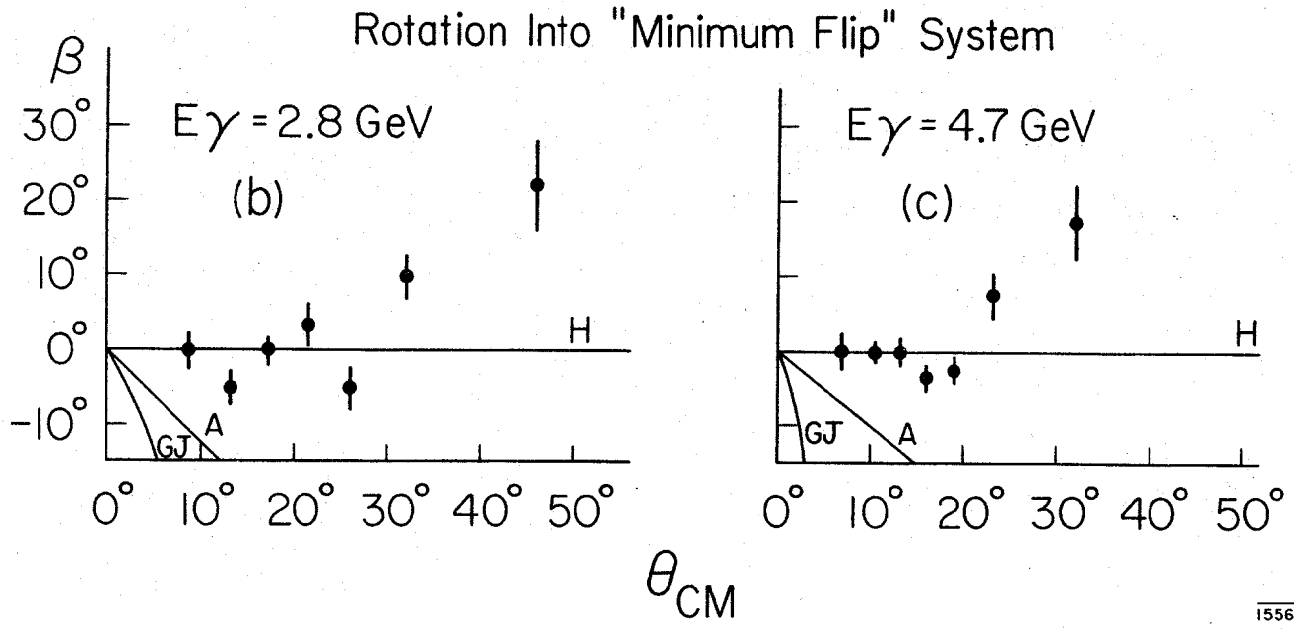
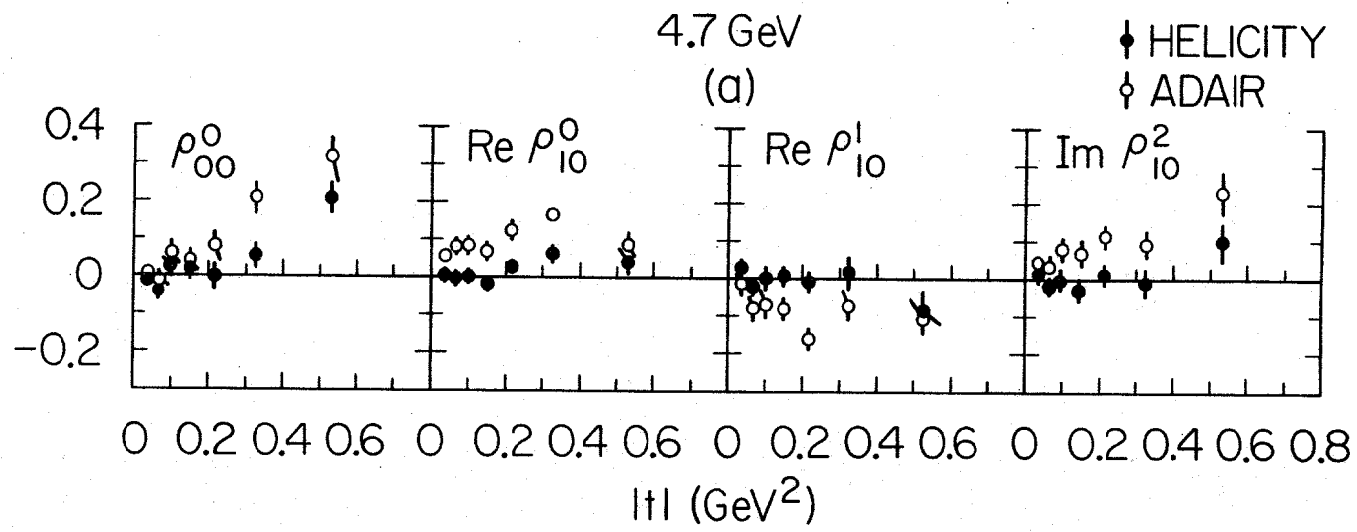


Fig. 4b



1556C5

Fig. 5